

Synthesis and Study of some Physical Properties of (CdO/NiO) Nanocomposite via Sol-Gel Method and their Antibacterial Activities

Amatalkareem Mohammed Al-Jezbi

Department of Physics, Faculty of Applied Science, Thamar University, Dhamar, Yemen

DOI: <https://doi.org/10.56807/buj.v4i2.307>

Abstract

The NiO and CdO nanoxides as well as the CdO/NiO oxides mixture were prepared in five samples with different concentrations where the ratio of CdO/NiO was [(1: 0), (3: 1), (1: 1), (1: 3), (0: 1)] by using the gel solution using a polyvinyl alcohol solution (PVA) and the samples were platelimed at (500°C) for three hours. The structural properties of the prepared oxides resulting from the cracking process were studied. The XRD results show the presence of pure cadmium oxide diffraction patterns in the sample (S₁) as well as the pure nickel oxide in the sample (S₅) and confirm the presence of the CdO / NiO oxide mixture in the samples (S₂, S₃, S₄). The results of XRD also show, through calculations, that the specific surface area increases with increasing granular size and decreases with decreasing granular size. XRD calculations also show that the intensity of eruptions decreases as the granular volume increases and increases with decreasing granular size. Optical measurements were taken and absorption spectra *at wavelength (215 nm) within the UV range*. The results of the optical measurements show an increase in the energy gap of the mixture. Samples were taken for continuous electrical conductivity measurements. It was found that the highest conductivity was the sample (S₃) which reached (0.394 S / cm), and the biological efficacy sensitivity of the samples was tested on six types of bacteria. The samples show varying efficacy on the six types, all of which were highly influencing the samples of the bacteria under study.

Keywords: Antibacterial, Oxide mixed, Optical, Electrical and Cadmium Oxide.

1. Introduction

Nanoscale semiconductors are characterized by unique characteristics and special properties in the field of Nano. Due to the development of modern technology, nanotechnology has become at the forefront of the most important fields and the widespread interest in nanotechnology dates back to 1996 - 1998, where particles less than 100 nanometers in size give the substance, which is included in its composition new properties. Transparent Conductive Oxides (TCO) materials that are semiconductor compounds made of metal with low dimension oxygen showed an enormous ability to solve most issues, such as developing sensor systems, producing antibiotics, developing transistors and other issues that these oxides were able to overcome and find appropriate solutions to them. Oxide compounds are of great importance in terms of the multiplicity of scientific fields involved in their development. The researchers were interested in developing them and producing new oxide materials or developing discoveries from them through conducting various vaccinations for them. Metal oxides are very important in the manufacture of materials needed for development in various fields of science, where studies focused on knowing the different properties of oxide compounds that were prepared using different methods such as the method of microwave deposition as well as the method of self-building, etc. Previous studies focusing on the oxide mixture (NiO / CdO) as well as other metal oxides have achieved significant success in many applications in both the technological and biological fields (Karthik et al. 2018a).

The nickel nanoparticle oxide is a pale green solid nano-particle oxide that dissolves in solutions and alcohol of type P and has a cube crystalline structure (1-6b), possessing a high-energy gap of (3.5-4 eV) (Bahadur et al. 2008).

Nickel oxides and their atoms have been studied extensively in the past few years, have high electrical conductivity and have ferro-magnetic properties at high temperatures (Zhang 2010).

Metal oxides are very important in the manufacture of materials needed for development in various scientific fields. Studies focused on investigating the different properties of oxide compounds prepared using different methods, such as microwave deposition, self-building, etc. Previous studies focusing on the oxide mixture (NiO / CdO) as well as other metal oxides have achieved significant success in many applications in the technological. (Karthik et al. 2018a). Nickel oxide (NiO) is a semitransparent p-type semiconducting material with band gap width of about 3.8 eV (AI et al. 2008). It shows attractive electric (I et al. 1998), electrochromic (AZENS et al. 1998) and thermoelectric (SHIN and MURAYAMA 2000) properties as well as high chemical resistance. It is used as gas sensors or developed to fabricate photodetectors (LEONG-M. et al. 2005). Lately there has been a lot of interest in nickel oxide's optical and electrochromic properties connected with its possible application in displays and "smart windows". Especially semiconducting NiO films would be usefully applied in UV detection (OHTA et al. 2003), if these could reveal both satisfactory transmittance at the level of 80% and conductivity above 1 Scm^{-1} . Cadmium oxide CdO is one of transparent conducting oxide materials whose thin films are regarded as a material with many attractive properties such as large energy band gap, high optical transparency in the visible spectral region, remarkable luminescence characteristics etc.. Due to these properties CdO is a promising material for electronic or optoelectronic application, such as solar cells application, photodiodes and gas sensors (Nasera et al. 2013).

Alcohol of type P and has a cube crystalline structure (1-6b), possessing a high-energy gap of (3.5-4 eV) (Bahadur et al. 2008). Nickel oxides and their atoms have been studied extensively in the past few years and have shown to possess high electrical conductivity and ferromagnetic properties at high temperatures (Zhang 2010).

The cadmium nanoparticle oxide is a solid dark brown nanoparticle oxide that dissolves in water, is a semiconductor of type N, and has a cubic centered crystal-shaped structure. It also has an

at (2.4 eV). High electrical conductivity and has potential applications on display, optical devices and other applications. Polyvinyl alcohol (PVA) is of interest because of its simple processing, high transmittance and it is easily soluble in water so it has numerous applications in polymer engineering technology, pharmaceutical and biomedical applications (Kim and Hyun 2003; Zhang FM et al. 2010). The study claimed the enhanced thermal stability of PVA/nanocomposites as compared to the pure PVA (Lagashetty;A. et al. 2009). is the most

Material	Company	molecular weigh	Purity
[Ni(NO3)2.6H2O]	(Sigma-Aldrich)	290.81	%98
[Cd(NO3)2.4H2O]	(Sigma-Aldrich)	308.47	%98
(PVA)	(Sigma-Aldrich)	72000	%98
(H2O)	Yamco	-	%99

energy gap in the visible spectrum region located

widely

reported technique. Beads free PVA based CdO nanofibers were synthesized by electrospinning technique. In general, PVA is most-widely used polymer for various precursor salt due to its good water solubility nature (Koski et al. 2004), hydrophilic nature (Gao et al. 2013) of PVA polymer gives excellent chemical and thermal stability with different metal salts. Furthermore, PVA also exhibits semicrystalline, which is a good sign for synthesizing crystalline nanofibers (Thomas et al. 2018).

The cadmium nanoparticle oxide is a solid dark brown nanoparticle oxide that dissolves in water, is a semiconductor of type N, and has a cubic centered crystal-shaped structure. It also has an energy gap in the visible spectrum region located at (2.4 eV). High electrical conductivity and has potential applications on

display, optical devices and other applications

2. Experimental details

2.1. Materials

2.2. Synthesis of (NiO/CdO) nanocomposite

Polymer (PVA) (5 g) was dissolved in 500 ml of distilled water at a temperature of 80 °C for 8 hours. The following relation was used to calculate the required weights:

$$W = \frac{M \cdot V \cdot M_{wt}}{1000} \dots(1)$$

In which W denotes weight, M is molarity, V is solvent volume, M_{wt} is molecular weight. The dissolved polymer was divided into five with a fixed volume of 40 ml per baker. The double addition of aqueous nickel nitrate and aqueous cadmium nitrate was carried out in two steps:

The nitrate solutions were prepared separately by dissolving them in a fixed volume of distilled water ((10 ml with different molar concentrations. Double mixing of a fixed volume of polyvinyl alcohol (PVA) (40 ml) with the prepared solutions shown in the previous table of cadmium nitrate and aqueous nickel nitrate for the five samples with constant stirring at a

constant temperature of 40 °C for 20 minutes, after which these samples were dried and poured in the dishes of Petri Dash. Then it is inserted into the drying oven at a temperature of 70 °C for a period of 5 hours to obtain the compound $[\text{Cd}(\text{NO}_3)_2 \cdot 4\text{H}_2\text{O}] \setminus \text{PVA} \setminus [\text{Ni}(\text{NO}_3)_2 \cdot 6\text{H}_2\text{O}]$ as flexible transparent disks. The Model LDO-080N CERTIFIED, a drying oven of the Faculty of Applied Sciences, was used to dry the prepared samples, heating them to the required temperature to get rid of the water and obtain solid samples within a short period of time. Finally, the prepared samples were platelimed at a temperature of 500 °C to obtain the nanoxide mixture (NiO/CdO) from the prepared samples with their different concentrations.

3. Results and discussion:

3.1 . X-ray diffraction (XRD):

That have been prepared, and through which can know the crystal structure of the different elements and compounds. Fig. (1) shows clear reflections of X-ray diffraction for cadmium oxide and nickel oxide in the samples prepared (S₁), (S₂), (S₃), (S₄), (S₅) prepared in a fixed volume of polyvinyl alcohol at 5

concentrations. Molarity is different [(1:0),(3:1),(1:1),(1:3),(0:1)].

Fig. (1) shows diffraction patterns for the samples (S₁), (S₂), (S₃), (S₄) at the crystalline levels (111), (200), (220), (311) and (222) for the corresponding angles (2θ), respectively (33°), (38.3°), (55.5°), (66.2°), and (69.56°), and this indicates the presence of Cadmium (CdO) with a cubic structure that exactly matches the card (JCPDS) No. (0.5- 064) which confirms that the (CdO) sample is a face centered cubic (FCC) structure (yufanyi et al. 2014).

Fig. (1) also shows diffraction patterns for the samples (S₂), (S₃), (S₄), (S₅) at the crystalline levels (111), (200) and (220) for the corresponding angles (2θ), respectively (37.2°), (43.2°) and (62.98°). This indicates the presence of nickel oxide (NiO) with a cubic structure that is in perfect conformity with the card (JCPDS) No. (47-1049) which confirms that the NiO sample is a cube crystal structure (Karthik et al. 2018a). In Fig. (1), we notice the appearance of diffraction patterns of the transition element (Ni) in the samples (S₄) and (S₅), due to the high percentage of nickel nitrate in the two samples during preparation.

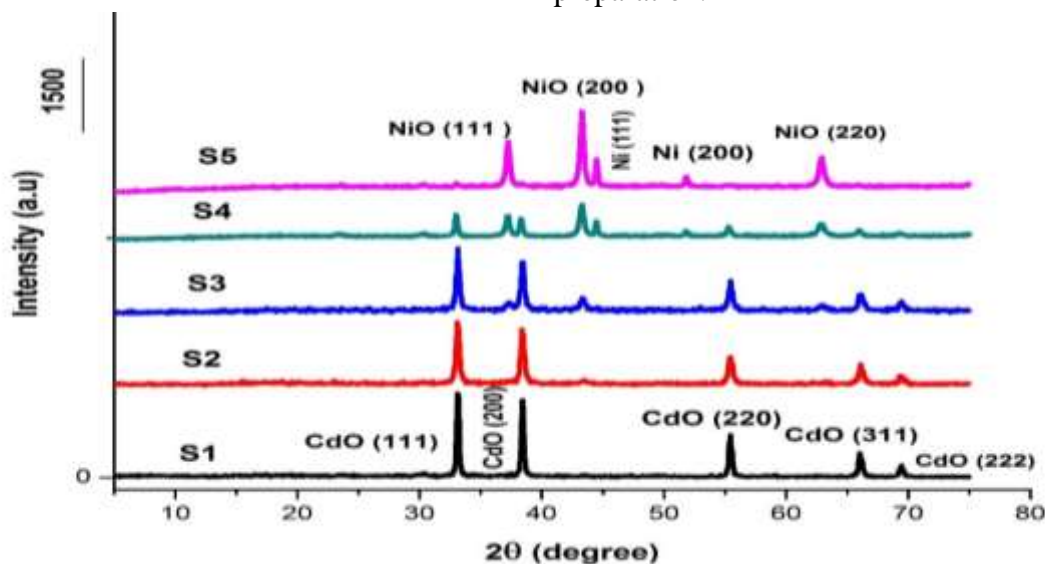


Fig. (1) X-ray diffraction patterns for the prepared samples

To calculate the reticular constant (a_{hkl}) in Table (1) of Cadmium Oxide and Table (2) of Nickel Oxide, the following relation was used:

$$a_{hkl} = d_{hkl} \sqrt{(h^2 + k^2 + l^2)} \quad \dots (2)$$

in which (a_{hkl}) denotes the Miller coefficients for crystalline levels, (d_{hkl}) the distance between the crystalline levels.

The Hall equation was used to calculate the grain size of the samples under study:

$$\beta \cos\theta = 2\eta \sin\theta + \frac{\lambda}{t} \quad \dots (3)$$

By drawing the graph between ($\beta \cos\theta$) on the axis (y) and ($\sin\theta$) on the x axis). Then, (Origin lab8) application was used to find the best straight line that passes through most points using the (Linear fitting) command so that it is found the point that the straight line crosses in the axis (y) through the equation (3), then this point is given by the value $y = \lambda / t$. By knowing the point, the granular size (t) can be calculated as shown in Table (1) and Table (2). The sample surface area (SSA) of nickel oxide in Table (1) and cadmium oxide in Table (2) was calculated using the following relation (Li. et al. 2003):

$$SSA = \sqrt{3} a^2 \frac{N_A}{M_{wt}} \quad \dots (4)$$

in which M_{wt} denotes the molecular weight of cadmium oxide ($M_{wt} = 128.41$ g / mol), and nickel oxide ($M_{wt} = 74.6928$ g / mol), a reticular constant, N_A is the number of Avogadro ($6.022 * 10^{23}$).

The samples were also calculated by the dislocation density of cadmium oxide in Table (1) and nickel oxide in Table (2) through the relation (Karthik et al. 2018b):

$$\delta = 1/t^2 \quad \dots (5)$$

In which t denotes the grain size. The morphology index has also been calculated in Table (1) and Table (2) of Oxides by the following relation (Karthik et al. 2018b):

$$MI = \frac{FWHM_h}{FWHM_h + FWHM_p} \quad \dots (6)$$

In which: $FWHM_h(\beta)$: is the highest value of the diffraction pattern width at half the value of the maximum intensity. $FWHM_p(\beta)$: The angle value of the diffraction pattern width at half of the maximum intensity value per pic. Tables (1) and (2) show the XRD-theoretical density values that were found using the following relation (Farooq et al. 2013):

$$\rho_m = 8M_{wt}/N_A a^3 \quad \dots (7)$$

In which M_{wt} denotes molecular weight, N_A is number of Avogadro, a reticular constant.

Table (1) XRD Calculations of cadmium oxide for Prepared Samples

Samples	Planes	Average Of Lattice Constant (a) Å	Specific Surface Area (SSA) (m ² /g)	Grain Size (t) (nm)	Morphology Index (MI) Rad	Dislocation density ($\delta \cdot 10^{15}$) (1/m ²)	XRD-theoretical density (ρ_m) (g/cm ³)
S₁	Plane(111)	4.686	1783.64	34.61	0.0087	0.834	16.578
	Plane(200)				0.0087		
	Plane(220)				0.0084		
	Plane(311)				0.0080		
	Plane(222)				0.0079		
S₂	Plane(111)	4.6857	1783.28	27.75	0.0077	1.298	16.581
	Plane(200)				0.0076		
	Plane(220)				0.0073		
	Plane(311)				0.0071		
	Plane(222)				0.0066		
S₃	Plane(111)	4.6855	1783.38	28.57	0.0077	1.225	16.584
	Plane(200)				0.0076		
	Plane(220)				0.0073		
	Plane(311)				0.0068		
	Plane(222)				0.0066		
S₄	Plane(111)	4.6912	1787.62	34.73	0.0083	0.888	16.523
	Plane(200)				0.0088		
	Plane(220)				0.0080		
	Plane(311)				0.0076		
	Plane(222)				0.0077		

Table (2) XRD Calculations of Nickel Oxide for Prepared Samples

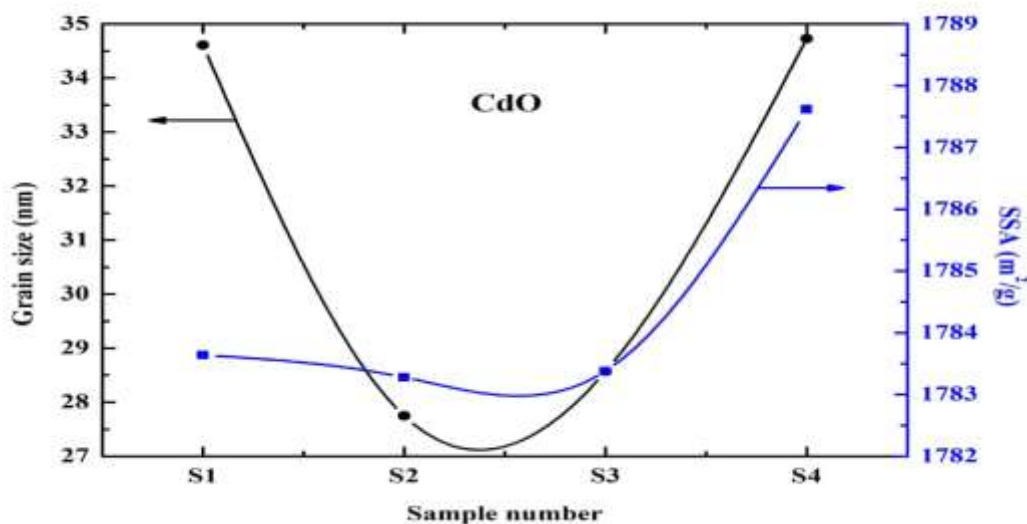
Samples	Planes	Average Of Lattice Constant (a) Å	Specific Surface Area (SSA) (m ² /g)	Grain Size (t) (nm)	Morphology Index (MI) Rad	Dislocation density ($\delta \cdot 10^{15}$) (1/m ²)	XRD-theoretical density (ρ_m) (g/cm ³)
S₂	Plane(111)	3.3528	1569.76	13.21	0.00665	5.730	26.33
	Plane(200)				0.00745		
	Plane(220)				0.00744		

S ₃	Plane(111)	3.3603	1576.85	14.60	0.00661	4.691	26.15
	Plane(200)				0.00715		
	Plane(220)				0.00685		
S ₄	Plane(111)	3.3651	1581.30	52.74	0.00858	0.36	26.04
	Plane(200)				0.00839		
	Plane(220)				0.00703		
S ₅	Plane(111)	3.3643	1580.59	39.59	0.00879	0.638	26.06
	Plane(200)				0.00872		
	Plane(220)				0.00767		

Through the results in the above table, the morphology of the surface, the intensity of the dislocation, and the specific surface area were calculated, as we note that the qualitative surface area increases mostly with increasing granular size and decreasing with decreasing granular size. In contrast, the ratio of the surface area to volume will increase with the decrease in the granular volume in both oxides, and the intensity of the

eruptions decreases with the increase in the surface area of the surface and increase with the decrease in the surface qualitative area of the surface (Ghiyasiyan-Arani et al. 2017). The value of the grid constant is consistent with previous studies. It was also found that the severity of the dislocation decreases as the granular size increases and increases with decreasing granular size (Karthik et al. 2017).

The figure below shows the relation between the SSA and the granular size on the vertical axis relative to the samples on the horizontal axis as in the Fig (2).



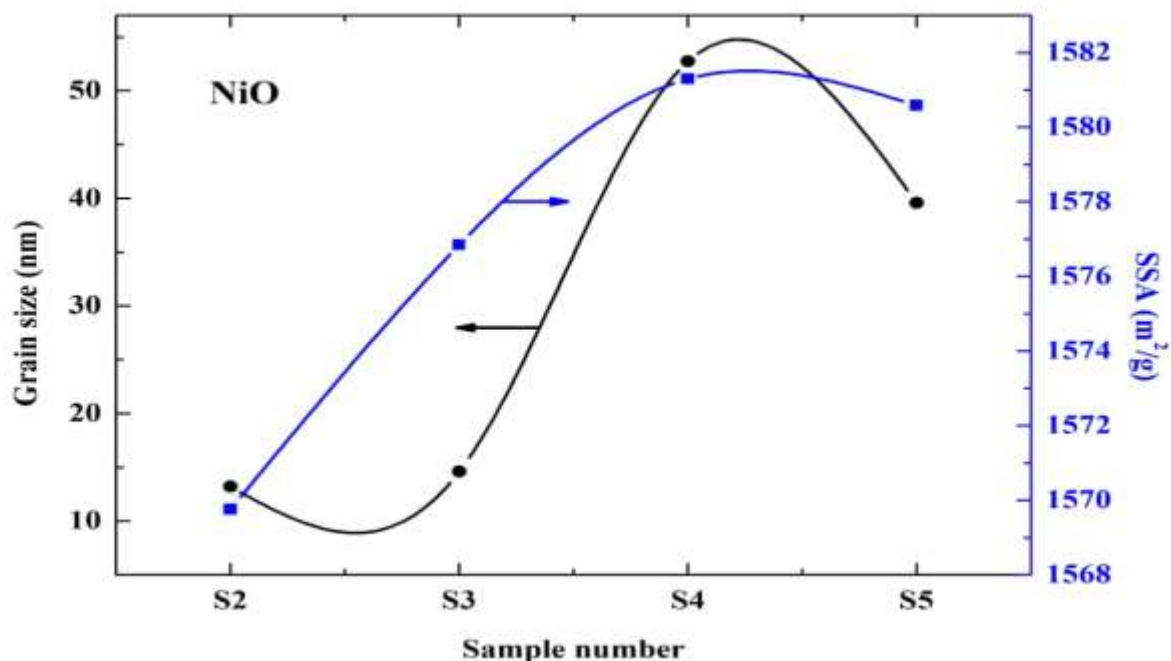


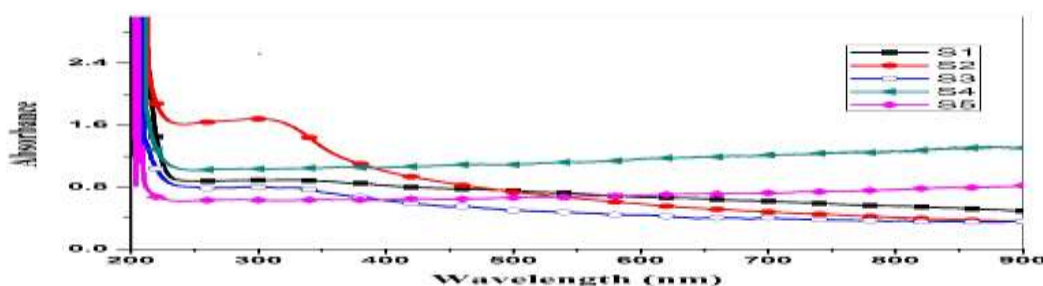
Fig (2) shows the relation between the SSA and the granular size

3.2. Optical Properties

Optical measurements of the oxide samples produced after drying and cracking have been performed at a temperature of 500°C, where absorption spectra of (CdO), (NiO) and (CdO / NiO) are indicated as shown in Fig (3).. The absorption and permeability spectra at

wavelengths (215 nm) indicate within the ultraviolet range (190-380nm). Therefore, oxide compounds can be used as a UV protector with lengths less than (215 nm) because the compounds have the ability to absorb them and do not allow their passage.

Fig (3-a) shows Absorbance and Transmittance for samples after Combustion



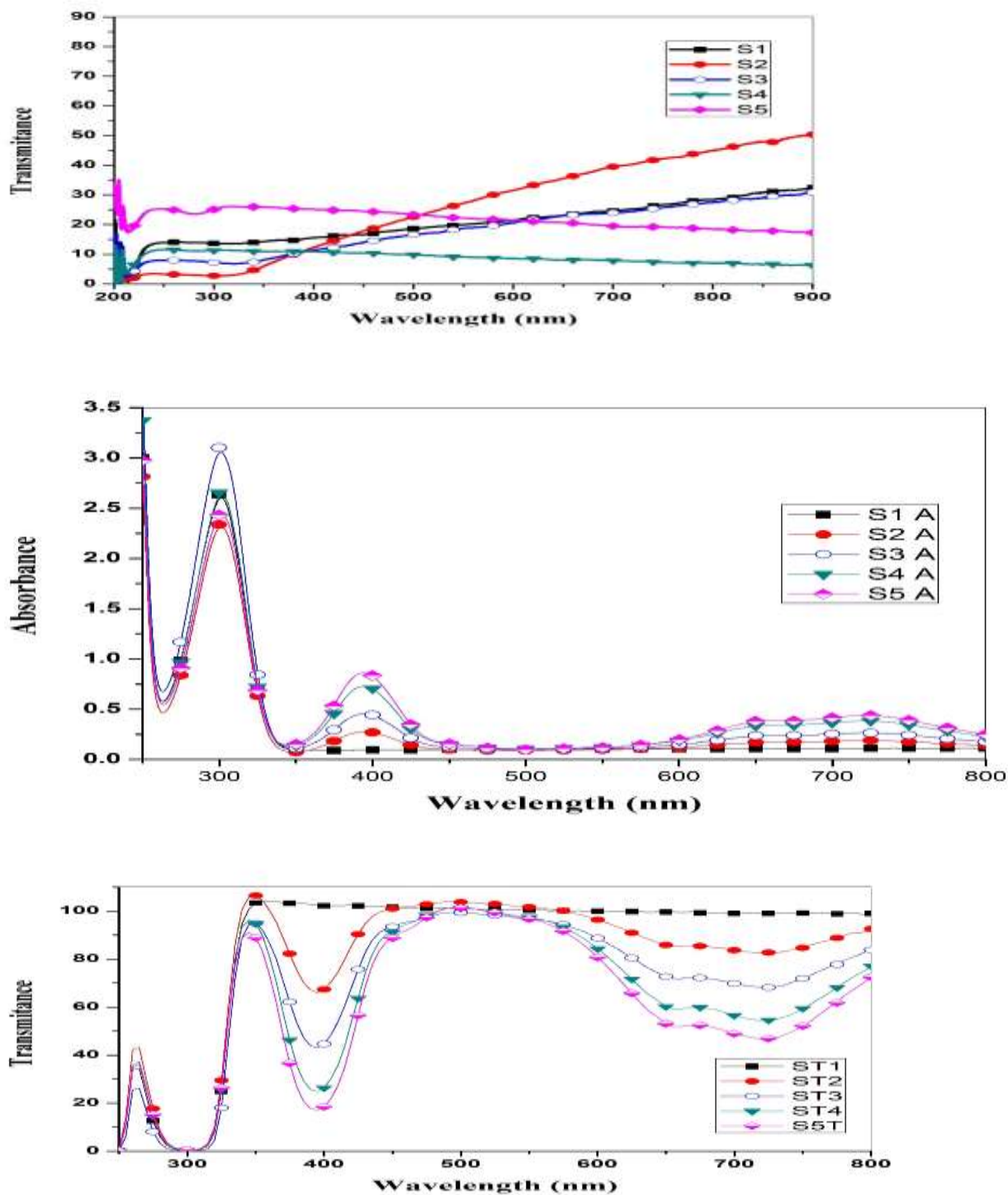


Fig (3-b) shows Absorbance and Transmittance for samples before Combustion

When a nano-semiconductor (CdO) is formed, the electrons of the (CdO) move from the valence band into the conduction band i.e. from $[(4d^{10})$ of (Cd) or from $(2P^6)$ of (O)] to the conduction band (Al-Huda et al. 2016). In the

same way for (NiO), electrons move from $[(3d^8)$ of (Ni) or from $(2P^6)$ of (O)] to the conduction band and thus absorb as a result of the transition of electrons between energy levels occurs. Whenever the number of electrons large

the absorption is higher. The energy gap for direct transmission was calculated by the relation (Karthik et al. 2018a):

$$(\alpha \cdot hv)^2 = c(hv - E_g) \quad \dots (8)$$

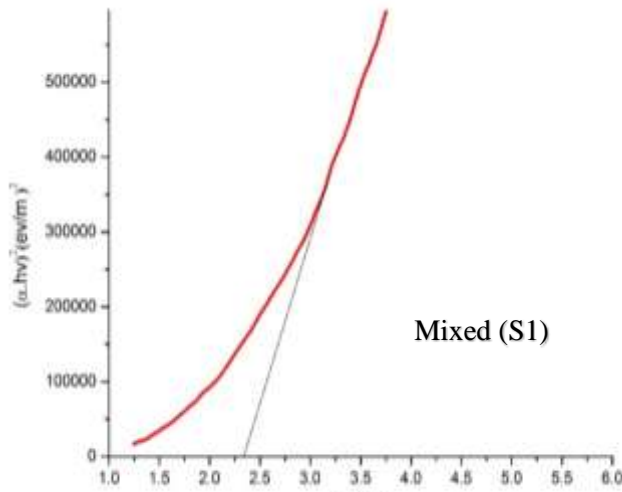
In which E_g denotes the energy gap for direct transmission, c is constant depends on the type of semiconductor, α is absorption coefficient and given by the following relation:

$$\alpha = 2.303 \frac{A}{d} \quad \dots (9)$$

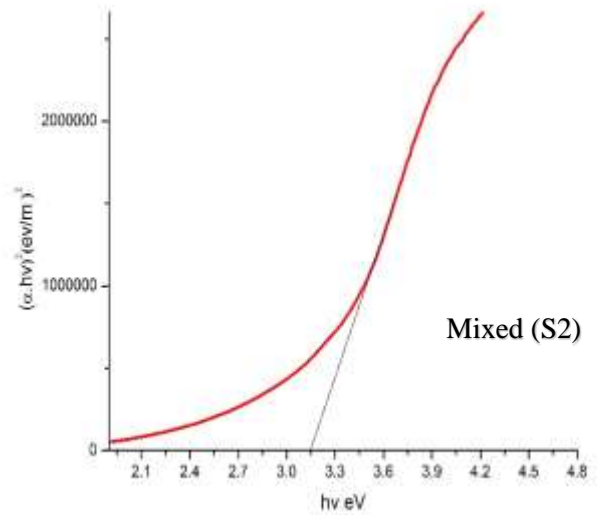
In which Absorbance of samples, d is cell thickness equals (1cm), hv is the photon energy and can be calculated from the following relation:

$$E = hv = hc/\lambda \quad \dots (10)$$

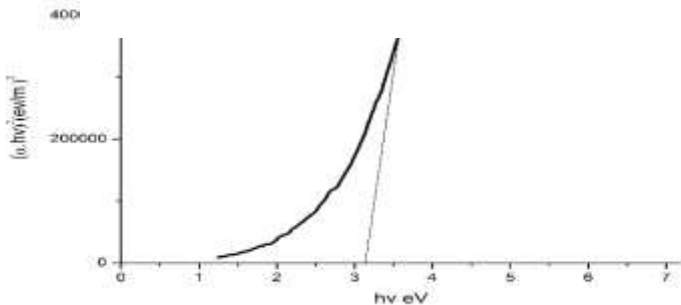
Where the absorbance coefficient was calculated for all absorbance values (A), and the photon energy was calculated from the relationship (10) for all wavelengths (λ) at which the absorbance was measured. The change between the left side of the equation (8) and the photon energy hv results in a curve formation group of points forms a straight line, When taking along these points straightening produces a straight line through the axis of hv value that intersects with this line represents the value of the energy gap E_g for the sample. The energy gap value was calculated for both CdO and NiO and for the mixture and was as shown in the following figures:



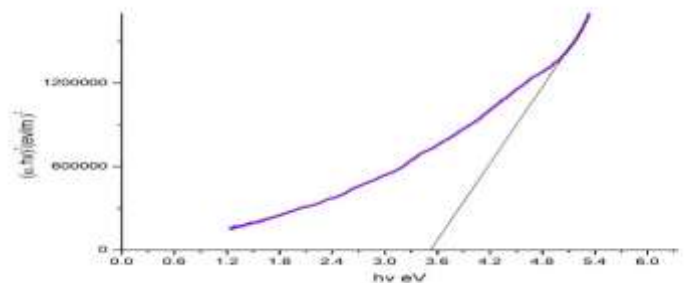
Shows the energy gap of cadmium oxide in the sample (S1).



Shows the energy gap in the sample S2



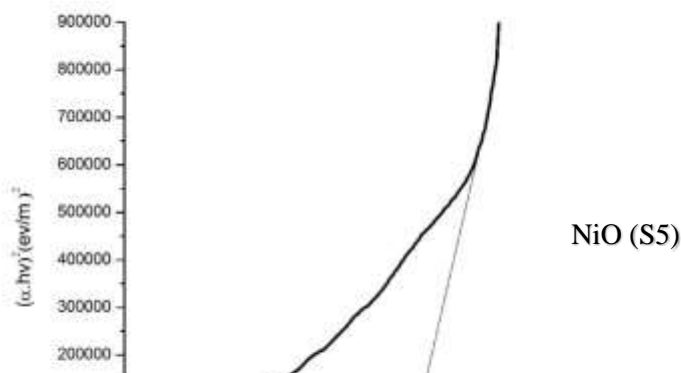
Mixed (S3)



Mixed (S4)

Shows the energy gap in the samples S3

Shows the energy gap in the sample S4



Shows the energy gap in the sample S5

The following table shows the energy gap for the prepared oxides (CdO), (NiO), (CdO / NiO) in samples (S₁, S₂, S₃, S₄, S₅):

Table (3) Energy Gap Calculations

Energy Gap Values					
Samples	S ₁	S ₂	S ₃	S ₄	S ₅
CdO	2.4	-	-	-	-
Mixed	-	3.15	3.2	3.5	-
NiO	-	-	-	-	4.4

From the above results, we notice an increase in the energy gap of the samples. The increase in the energy gap is due to the discordant interaction between the unfilled states at the lowest edge of the conduction band of the CdO with the highest edge of the valence band of (NiO) which is the donor-like level of (CdO) as a result of mixing. The higher the (NiO) concentration inside the sample, the more electrons are at the d-level.

Thus, the repulsion between the electrons of the lowest conduction band of the CdO and electrons of the highest valence band for (NiO) Which increases the widening energy gap of the mixture (Francis et al. 2015). We also notice an increase in the energy gap of (CdO) and (NiO), and this may be caused by the occurrence of quantitative restriction of samples

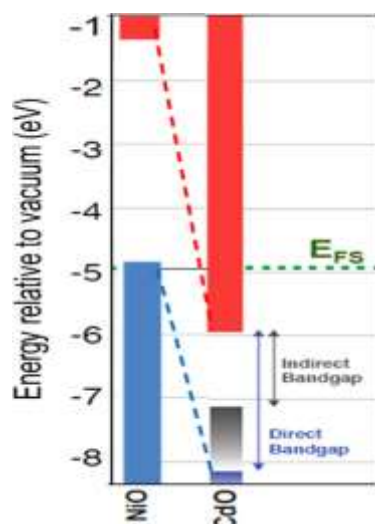


Fig. (5) Shows the repulsive reaction when mixing oxides

4.3 Results Of Continuous Electrical Conductivity (σ_{DC})

Continuous electrical conductivity measurements were performed for the samples prepared before and after cracking at (500 °C) as shown in Table (4) and Fig. (6). The table and figure note the behavior of continuous electrical conductivity (σ_{DC}).

Table (4) values of electrical conductivity of prepared samples

Sample	Electrical Conductivity ($10^{-3} * \sigma_{DC}$) Before Cracking Process	Electrical Conductivity ($10^{-3} * \sigma_{DC}$) After Cracking Process
S ₁	25.8 (S/cm)	382 (S/cm)
S ₂	26.3 (S/cm)	392 (S/cm)
S ₃	31.6 (S/cm)	394 (S/cm)
S ₄	28.8 (S/cm)	386 (S/cm)
S ₅	26.9 (S/m)	384 (S/cm)

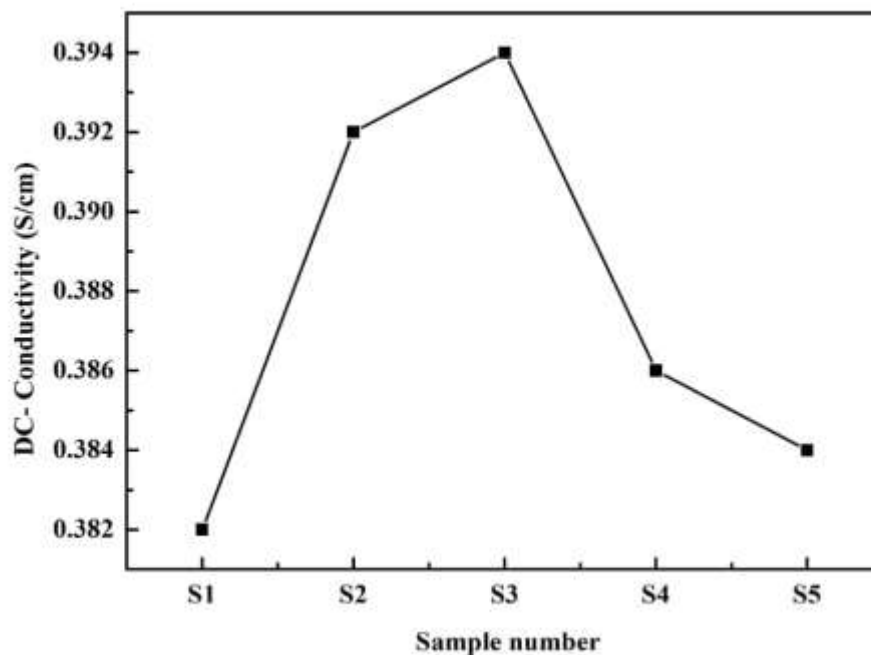


Fig. (6) shows continuous electrical conductivity behavior of prepared samples after cracking

Continuous electrical conductivity (σ_{DC}) exhibits a general behavior in the gradual increase with a mixing ratio of Cd: Ni until it reaches its highest value at the ratio of Cd: (Ni (1: 1) and then begins to decrease. We observe through the measurements where (NiO) of P-type and n-type CdO. We notice an increase in the value of electrical conductivity with an increase in the concentration of nickel oxide to cadmium oxide. That is, the conductivity increases with an increase in the concentration of positive charge carriers (gaps) when there are sufficient electrons resulting from a high concentration of cadmium oxide, and when the concentration of both nickel oxide and cadmium oxide is equal in the S3 sample we get. It has the highest value of electrical conductivity (0.394 S / cm). That is, when the concentration of negative charge carriers (electrons) in cadmium oxide and positive charge carriers (gaps) in nickel oxide are equalized, we get the highest value of electrical conductivity. Then that with an increase in the concentration of nickel oxide and a decrease in

the concentration of cadmium - due to the difference in the concentration ratios - the positive charge carriers increase the and decrease the negative charge carriers with it, which leads to a decrease in the value of electrical conductivity .

4.4.1 Effect of the prepared oxides on six types of bacteria

In this study, the sensitivity of the prepared oxides (CdO), (NiO) and (CdO / NiO) was tested on six types of bacteria, namely:

- Escherichia Coli): It is one of the most prevalent species and is found naturally in the colon for humans and some animals. However, there are strains of them that cause humans many diseases, some of which are fatal, including the Enterohaemorrhagic E. coli strain that causes bloody colitis (HC). In all ages without a fever, this strain can cause urinary tract infections with kidney failure, so it is classified as the most dangerous strain (E. coli).
- (Salmonella): It is one of the types of bacteria spread widely in remote societies. There are

many diseases caused by this type of bacteria, including intestinal fever (typhoid), which is accompanied by germs in the blood and is present in the feces of the sick and pregnant person or contaminated water or by contamination of hands.

- (Klebsiella): It is a bacterium that possesses many strains that cause many diseases, including the strain (K.pneumoniae), which is one of the main causes of pneumonia. As a result, there is an abscess and can cause urinary tract infection and sepsis.

- (Staphylococcus aureus): This bacterial type causes several infections, including wound inflammation, pimples, ulcers, inflammation of burns and other diseases affecting the skin. It also causes meningitis, dermatitis and food poisoning with rapid symptoms without fever.

- (Streptococcus pyogenes): Streptococcus pyogenes is a type of positive bacterial bacterium, has an important role in skin diseases that affect humans, but infection is rare, but it is usually pathogenic even though it occurs naturally as part of the flora of the skin.

- (Pseudomonas aeruginosa): are bacteria that have the ability to cause disease states, including meningitis, and what is fatal, such as erosion of the lungs, and is characterized by its high ability

to resist many antibiotics, which complicates the treatment of infections of this type of bacteria.

After the medium was prepared from (Hueller Hinton Agar) bacteria were developed at conditions suitable for their growth and the effect of the oxides under study was determined with three different weights (1mg, 1.5mg, 2.5mg), the inhibition diameter was recorded for them and the results were as shown in the table and the figure. Through the results shown above, we note the high effectiveness of the sample (S1) on the bacteria (Streptococcus pyogenes), in which the inhibition diameter reached (25 mm), while the sample (S2) was the most influential on the bacteria (Klebsiella) and in which the inhibition diameter reached to (25 mm). The sample (S4) was the most influential on the bacteria (Escherichia Coli), where the diameter of its inhibition was (27 mm). Whereas it is noted through the results that the sample (S5) **was the highest impact** on the bacteria (Staphylococcus aureus), where the inhibition diameter reached it (25 mm), for the sample (S3) was effective on three types of bacteria (Klebsiella) and (Streptococcus pyogenes) as well as (p. aeruginosa).

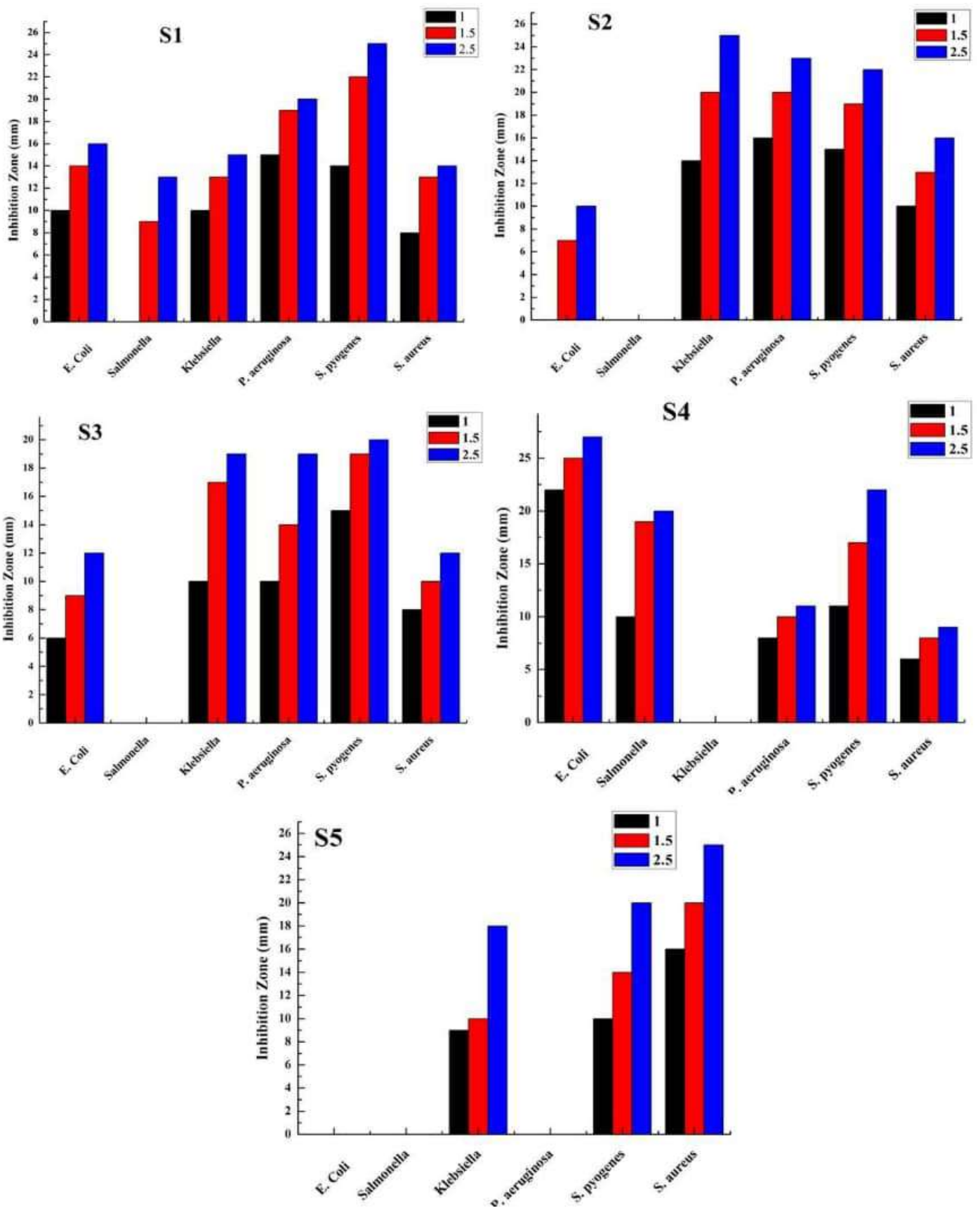


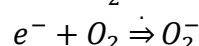
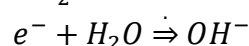
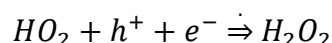
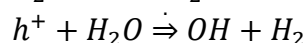
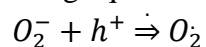
Table (5) Effect of prepared oxides on six types of bacteria

<i>Klebsiella</i>			<i>Salmonella</i>			<i>Escherichia Coli</i>			Simple
2.5 (mg)	1.5 (mg)	1 (mg)	2.5 (mg)	1.5 (mg)	1 (mg)	2.5 (mg)	1.5 (mg)	1 (mg)	
15	13	10	13	9	R	16	14	10	S1
25	20	14	R	R	R	10	7	R	S2
19	17	10	R	R	R	12	9	6	S3
R	R	R	20	19	10	27	25	22	S4
18	10	9	R	R	R	R	R	R	S5

<i>S.aureus</i>			<i>S.pyogenes</i>			<i>p. aeruginosa</i>			Simple
2.5 (mg)	1.5 (mg)	1 (mg)	2.5 (mg)	1.5 (mg)	1 (mg)	2.5 (mg)	1.5 (mg)	1 (mg)	
14	13	8	25	22	14	20	19	15	S1
16	13	10	22	19	15	23	20	16	S2
12	10	8	20	19	15	19	14	10	S3
9	8	6	22	17	11	11	10	8	S4
25	20	16	20	14	10	R	R	R	S5

Mechanism of action (CdO / NiO) as an antibiotic:

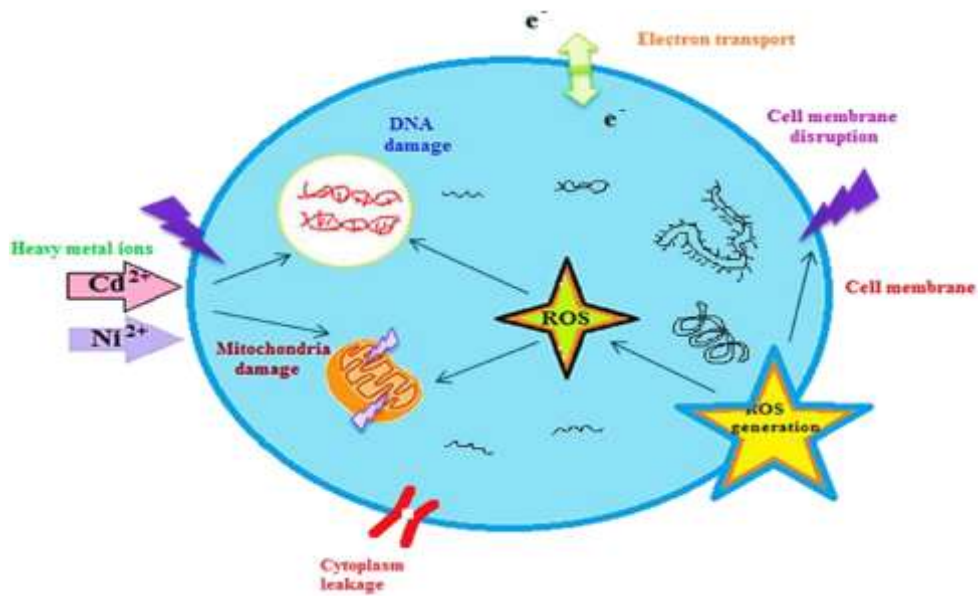
After adding the nano (CdO / NiO) and under the influence of (UV) present in the normal light, it gets excited by the electrons, where (CdO / NiO) absorbs photons coming from light, especially the small wavelengths near the color blue and ultraviolet produces a pair (electron-gap) and begins crossing into the bacterial cell. Since water is an essential component of the bacterial cell, (electrons and gaps) interact with water forming active oxygen cutting compounds (ROS) which are three compounds (OH, O₂, H₂O₂) produced within the cell according to the following equations:






In addition, it also produces (OH⁻) (H₂O₂⁻) (O₂⁻) compounds that work on the outer cell wall only because they cannot penetrate due to their negativity while the bacterial cell wall is always negative. Because (Cd⁺) and (Ni⁺) are positive, they interact electrostatically with the negative cell wall and stick to it, since the cell membrane includes in its composition (Thiol groups) that are bound to the ends on the outer surface of the membrane called groups (SH⁻), these groups will interact with ions (Cd⁺) and (Ni⁺) and this leads to destruction. These groups damage the cell membrane and make it easier for (Cd⁺) and (Ni⁺) ions to penetrate, as they stop their

functions in cellular respiration, which negatively affects the DNA replication and bacterial cell division, leading to oxidative stress and thus the

Bacterial cell dies as shown in the following figure



<i>Escherichia Coli</i>	<i>Salmo nell</i>	<i>Klebsiella</i>
		
<i>S.aureus</i>	<i>S.pyogenes</i>	<i>p. aeruginosa</i>



Conclusions:

X-ray diffraction show several results, the most important of which are:

- The presence of diffraction patterns for the transition element (Ni) in the two samples (S4) and (S5), due to the high percentage of nickel nitrate in the two samples during preparation.
- Through calculations it was found that the specific surface area increases with increasing granular size and decreases with decreasing granular size. On the other hand, the ratio of surface area to volume increased with decrease in granular size, and this is consistent with previous studies.
- It was found through the calculations that the intensity of the eruptions decreases as the granular size increases and increases with decreasing granular size.

The results of the optical properties study show the following:

- Absorption spectra appeared at the wavelength (215nm) within the ultraviolet range (190-380nm). Therefore, oxide compounds can be used as a UV protector with lengths less than (215nm) because the compounds have the ability to absorb them and do not allow their passage.
- An increase in the value of the energy gap of the mixture with an increase in the concentration (NiO). This is due to the incoherent reaction as a result of mixing. The energy gap for nickel oxide

and cadmium oxide has increased, due to the occurrence of quantitative restriction.

Measurement results for continuous electrical conductivity show that:

- When the concentration of negative charge carriers (electrons) in cadmium oxide and the positive charge carriers (gaps) in nickel oxide, we obtained the highest value of continuous electrical conductivity, which reached (0.394 S / cm).
- When you increase the concentration of nickel oxide and decrease the concentration of cadmium oxide - due to the different concentration ratios - the positive charge carriers increase and the negative charge carriers with them decrease, which leads to a decrease in the value of electrical conductivity.

- The results of the sensitivity test on six types of bacteria demonstrated varying efficacy of the samples in the six types, all of which were highly influencing all types of bacteria under study. The effect of the sample (S4) on the bacteria (E. coli) was the highest as the inhibition diameter reached (27 mm) and thus considered a good antidote to this type of bacteria.

Declarations

- Availability of data and materials: (Not applicable)
- Competing interests: (Not applicable)

- Funding:

(Not applicable):

- Authors' contributions:

Amatalkreem Mohammed Al-Jezbi designed the experiments, provided guidance and wrote the manuscript.

- Acknowledgements:

I thank Dr\ Abdullah Ahmed Ali Ahmed (Department of Physics, Faculty of Applied Science, Tamar University, Dhamar, 87246, Yemen) for supervising the preparation of research samples in the manuscript.

References

- Bahadur, J. and Sen, D. and Mazumder, S. and Ramanathan, S. (2008), 'Effect of heat treatment on pore structure in nanocrystalline NiO: A small angle neutron scattering study', *journal PRAMANA of physics*, 71, 6.
- Farooq, H. and Raza Ahmad, M. and Jamil, Y. and Hafeez, A. and Anwar, M. (2013), 'Structural, dielectric and magnetic properties of superparamagnetic zinc ferrite nanoparticles synthesized through coprecipitation technique', *Kovove Mater*, 51, 6.
- Francis, C.A. and Detert, D.M. and Chen, Guibin and Dubon, O.D. and Yu, Kin M. and Walukiewicz, Wladek (2015), 'NixCd1-xO: Semiconducting alloys with extreme type III band offsets', *APPLIED PHYSICS LETTERS*, 4.
- Ghiyasiyan-Arani, M. and Niasari, M.S. and Arani, M.M. and Mazloom, F. (2017), 'An easy sonochemical route for synthesis, characterization and photocatalytic performance of nanosized FeVO₄ in the presence of aminoacids as green capping agents', *Mater Sci: Mater Electron*, 12.
- Karthik, K. and Dhanuskodi, S. and Gobinath, C. and Prabukumar, S. and Sivaramakrishnan, S. (2017), 'Multifunctional properties of microwave assisted CdO–NiO–ZnO mixed metal oxide nanocomposite: enhanced photocatalytic and antibacterial activities', *Materials Science*, 13.
- Karthik, K. and Dhanuskodi, S. and Gobinath, C. and Prabukumar, S. and Sivaramakrishnan, S. (2018b), 'Nanostructured CdO–NiO composite for multifunctional applications', *ScienceDirect*, 112, 13.
- Li., Shu-Ping and Hou., Wan-Guo and Han., Shu-Hua and Li., Li-Fang and Zhao., Wei-An (2003), 'Studies on intrinsic ionization constants of Fe–Al–Mg hydrotalcite-like compounds', *Colloid and Interface Science*, 257, 6.
- yufanyi, D.M. and Tendo, J.F. and Ondoh, .M. and Mbadcam, J.K. (2014), 'CdO nanoparticles by thermal decomposition of a cadmium-hexamethylenetetramine Complex', *Materials Science Research* 3(3), 11.
- AI, LEI and FANG, GUOJIA and YUAN, LONGYAN and LIU, NISHUANG and WANG, MINGJUN and LI, CHUN and ZHANG, QILIN and LI, JUN and ZHAO, XINGZHONG (2008), 'Influence of substrate temperature on electrical and optical properties of p-type semitransparent conductive nickel oxide thin films deposited by radio frequency sputtering', *Applied Surface Science*, 254 (8), 10.
- AZENS, A. and KULLMAN, L. and VAIVARIS, G. and NORDBORG, H. and GRANQVIST, C.G. (1998), 'Sputter-deposited nickel oxide for electrochromic applications', *Solid State Ionics*, 3.

- I, HOTOVÝ and J, HURAN and J, JANÍK and A.P, KOBZEV (1998), 'Deposition and properties of nickel oxide films produced by DC reactive magnetron sputtering', 51 (2), 4.
- LEONG-M. and CHOI. and SEONGIL, IM. (2005), 'Ultraiolet enhanced Si-photodetector using p-NiO films', *Applied Surface Science* 244, 4.
- Nasera, Ghazi Y. and Rajab, Waleed N. and Farisc, Ali S. and Rahemd, Zenhe J. and Salihe, Mohammed A. and Ahmedf, Auday H. (2013), 'Some optical properties of CdO thin films', *Energy Procedia*, 36, 8.
- OHTA, H. and KAMIYA, M. and KAMIYA, T. and HIRANO, M. and HOSONO, H. (2003), 'UV-detector based on pn-heterojunction diode composed of transparent oxide semiconductors, p-NiO/n-ZnO', *Thin Solid Films* 445(2), 445 (2).
- SHIN, W. and MURAYAMA, N. (2000), 'High performance p-type thermoelectric oxide based on NiO', *Materials Letters*, 45 (6), 5.
- Gao, Q. and Takizawa, J. and Kimura, M. (2013), 'Hydrophilic non-wovens made of cross-linked fully-hydrolyzed poly(vinyl alcohol) electrospun nanofibers', *Polymer*, 54, 7.
- Ghiyasiyan-Arani, M. and Niasari, M.S. and Arani, M.M. and Mazloom, F. (2017), 'An easy sonochemical route for synthesis, characterization and photocatalytic performance of nanosized FeVO₄ in the presence of aminoacids as green capping agents', *Mater Sci: Mater Electron*, 12.
- Kim, GS. and Hyun, SH. J. (2003), 'Effect of mixing on thermal properties of aerogel-PVB composites', *Materials Science*, 38 (9).
- Koski, A. and Yim, K. and Shivkumar, S. (2004), 'Effect of molecular weight on fibrous PVA produced by electrospinning', *Mater. Lett*, 58, 5.
- Lagashetty; A. and Basavaraj; S. and Bedre; M. and J., Venkatarman; A. (2009), 'Metal oxide dispersed polyvinyl alcohol nanocomposites', *Metall Mater Sci* 51 (4), 10.
- Thomas, D. and Zhuravlev, E. and Wurm, A. and Schick, C. and Cebe, P. (2018), 'Fundamental thermal properties of polyvinyl alcohol by fast scanning calorimetry', *Polymer*, 137, 10.
- Zhang FM and Chang J and B., Eberhard (2010), 'Dissolution of poly(vinyl alcohol)-modified carbon nanotubes in a buffer solution', *New Carbon Mater*, 25 (4), 6.